Effect of electron correlations in Pd, Ni, and Co monowires

Małgorzata Wierzbowska[1], Anna Delin[2] and Erio Tosatti[1,3,4]
[1] *INFM DEMOCRITOS National Simulation Center, via Beirut 2–4, 34014 Trieste, Italy*
[2] *Materialvetenskap, Brinellvägen 23, KTH, SE-10044 Stockholm, Sweden*
[3] *International School for Advanced Studies (SISSA), via Beirut 2–4, 34014 Trieste, Italy*
[4] *The Abdus Salam International Center for Theoretical Physics (ICTP), Strada Costiera 11, 34100 Trieste, Italy*
(Dated: February 2, 2008)

We investigated the effect of mean-field electron correlations on the band electronic structure of Co, Ni, and Pd ultra-thin monatomic nanowires, at the breaking point, by means of density-functional calculations in the self-interaction corrected LDA approach (LDA+SIC) and alternatively by the LDA+U scheme. We find that adding static electron correlations increases the magnetic moment in Pd monowires, but has negligible effect on the magnetic moment in Co and Ni. Furthermore, the number of d-dominated conductance channels decreases somewhat compared to the LDA value, but the number of s-dominated channels is unaffected, and remains equal to one per spin.

PACS numbers: 75.75.+a, 73.63.Nb, 73.22.-f, 75.20.En, 75.15.Mb

I. INTRODUCTION

Nano- and molecular-sized components hold considerable promise as forming the platform for an entirely new type of hardware technology. In such a future technology, quantum effects inherent in these nano-objects might give rise to new functionalities, possibly resulting in a totally different design of the basic components in information technology from what we are used to today. An important category of systems is constituted by ultra-thin conductors and nanocontacts. The best known and most investigated systems in this class are carbon nanotubes and molecular conductors. Metallic nanowires are also of high interest, but much less studied. Ultimately thin nanowires, *i.e.* freestanding atomic chains hanging between tips, constitute a unique metallic structure where nanosize properties of matter can be tested. Unlike nanotubes, they are clearly transient objects, although for applications they could be stabilized, *e.g.* inside other nanostructures. Besides, their transient nature could itself be put to use.

Metallic nanowires are fabricated using a scanning tunneling microscope (STM) or an atomic force microscope tip. By forming a metallic contact between the tip and sample of the same metal as the tip, and then retracting the tip, a thin neck or wire may form by plastic deformation. Just before it breaks, the nanocontact may consist of a single atom, and under some circumstances and in some metals of a short single chain of atoms – a segment of monatomic nanowire.[1,2] A second way in which nanowires can be produced is inside a transmission electron microscope[3] (TEM). With the TEM beam, two nearby holes are burned in a thin metal film, close enough that the bridge between them narrows down spontaneously to form a nanowire. A third way to produce nanowires is via the mechanically controllable break junction technique.[4]

It was recently predicted that quantum confinement of the electronic states in metallic atomic chains should lead to a magnetic ground state, and to a superparamagnetic state at finite temperatures, in Ru, Rh, Pd, Os and Pt.[5,6,7,8] In the present paper, we build on those results, also stimulated by some recent intriguing experimental results indicating unexpectedly low fractional conductance through Co, Pd and Pt nanocontacts and nanowires observed at room temperature[9,10,11] (note however that at low temperature, the uncontaminated break junctions fail to show fractional conductance and even nanowires in the case group III and IV transition metals.[10]) Assuming that, as in the room temperature experiments, short nanowires could easily form at the nanocontact, we wish to explore the possible effects of strong correlations on the electronic structure of the wires, and if and in what way strong correlations might relate to these recent experimental results.

We will be concerned here only with those correlation effects that can be included within conventional Fermi liquid theory, where quasiparticle electronic bands replace the noninteracting electron bands, but can be treated as such in every other aspect. Thus, we will not be addressing at all the strongest kind of correlation effects, including Coulomb blockades and Kondo phenomena, probably more typical for quantum dots than for genuine metallic nanocontacts. The effects which we will address here still amount to a nontrivial renormalization of the electronic bands, which can however be treated by means of static mean-field theories such as LDA+U and LDA+SIC.

The electron bands in transition metal nanowires, especially the d bands, are considerably narrowed by the reduced one-dimensional coordination. Band narrowing is further enhanced under the strong tensile stress that brings the nanowires close to the point of breaking. It is well known that for narrow band systems, standard density functional theory (DFT) approaches[12] – notably the local density approximation (LDA) and generalized gradient approximations (GGA) – do not reproduce well the electronic localization within the polarized atomic shells. For that reason we find it relevant and instructive to investigate how extensions of DFT, devised specifically

to improve the mean field static description of electron-electron correlations, affect the electronic structure of strongly stretched monatomic wires. In particular, we will make use of the LDA+U approach[13] and the self-interaction corrected LDA (LDA+SIC) scheme.[14]

We may anticipate that with these corrections, the band structure near the Fermi level E_F, including bandwidths and splittings could be strongly altered. In that case also the channel number (number of propagating bands that cross E_F), their transmission, and in the end ballistic conductance might be sensitive to correlations. In this work, devoted to strictly ideal infinite monatomic nanowires, we will address the sensitivity of bands and channels, though clearly not of transmission, to strong (albeit for the time being statically described) electron-electron correlations.

II. METHOD

The geometry adopted for the calculation was a two-dimensional lattice of infinite ideal monatomic chains, with the spacing between chains large enough to make their interaction negligible.

We performed all calculations using the SIESTA-1.3 code.[15] The starting point is in all cases a local (spin) density approximation, L(S)DA, calculation. On top of that, we treat the effect of strong correlations by an extension of LDA, namely the LDA+U method[13] and the self-interaction (SI) corrected LDA approach (LDA+SIC).[14] The latter method is an approximated scheme to retain the exact exchange and it does not add any correlations; LDA+SIC even removes a part of correlations, *i.e.* self-correlations. Thus, the effect of SI correction may differ from the LDA+U result.

The LDA+U correction potential, $V^{\sigma}_{U,m}$, to the LDA Hamiltonian is diagonal, and defined as

$$\begin{aligned} V^{\sigma}_{U,m} &= U\sum_{m'}(n^{-\sigma}_{m'} - n^{-\sigma}_{d}) + \\ &\quad (U-J)\sum_{m'\neq m}(n^{\sigma}_{m'} - n^{\sigma}_{d}) + \\ &\quad (U-J)(\frac{1}{2} - n^{\sigma}_{d}), \end{aligned} \tag{1}$$

with n^{σ}_{d} being the average orbital occupation of the correlated shell calculated self-consistently from the orbital occupations n^{σ}_{m},

$$n^{\sigma}_{d} = \frac{1}{2l+1}\sum_{m} n^{\sigma}_{m} = \frac{1}{2l+1}N_d, \tag{2}$$

during the LDA+U iteration process. We use here for N_d the total actual occupation number of the polarization shell (for instance d-shell) rather than fixing n^{σ}_{d} at half occupation or using an average LDA occupation. Details and a test of this implementation are given in Ref. [16]. Our definition of the local occupations n^{σ}_{m} also differs from the Mulliken occupations $n^{\sigma,Mulliken}_{m}$ (Ref. [31]) as follows

$$n^{\sigma}_{m} = \sum_{\mu\nu} S_{m\mu} D^{\sigma}_{\mu\nu} S_{\nu m}, \tag{3}$$

$$n^{\sigma,Mulliken}_{m} = \sum_{\nu} D^{\sigma}_{m\nu} S_{\nu m}, \tag{4}$$

involving differently the density matrix $D_{\mu\nu}$ and the overlap integrals $S_{m\mu} = \langle m|\mu\rangle$ and $S_{\nu m} = \langle \nu|m\rangle$ for the basis functions μ and ν and the projector function m. Further discussion of the local occupation numbers is given in Appendix A.

The d-shell exchange parameter J was set to 1 eV in all calculations. Varying J in the range $0.5-1.5$ eV was seen to have only a very minor effect on the studied systems. Several values for the intra-atomic Coulomb parameter U in the range $3-9$ eV were tested in order to get a broad insight into the electron localization effects. Thus, we use U as a free parameter in our calculations, although it can in principle be calculated self-consistently. We did calculate U self-consistently for our nanowires using the constrained density functional method described in detail in Refs. [17] and [18], in addition to treating U as a free parameter. The results are detailed and critically assessed in Appendix A. However, an indiscriminate use of self-consistently calculated U parameters is not unproblematic. The LDA+U method has indeed had great success in describing systems with rather localized d electrons, for example the $3d$ oxide NiO, where the LDA+U gives the correct insulating ground state as opposed to standard LSDA. On the other hand, when the LDA+U method is applied to systems which are in effect not strongly correlated, for example TiO, it fails, at least when a self-consistently calculated U is used in the calculation.[13]

In the present implementation of the LDA+SIC scheme[19], we adopted a modified pseudo-SIC approach closely akin but not identical to that in Ref. [14].

The LDA+SIC correction matrix, $V^{\sigma}_{SIC,\mu\nu}$, to the LDA hamiltonian is given by

$$V^{\sigma}_{SIC,\mu\nu} = \sum_{i} \frac{\langle\mu|\gamma^{\sigma}_{i}\rangle\langle\gamma^{\sigma}_{i}|\nu\rangle}{C^{\sigma}_{i}}, \tag{5}$$

$$\gamma^{\sigma}_{i}(\mathbf{r}) = V^{\sigma}_{HXC}[\rho^{\sigma}_{i}(\mathbf{r})]\phi_i(\mathbf{r}), \tag{6}$$

$$C^{\sigma}_{i} = \langle\phi_i|V^{\sigma}_{HXC}[\rho^{\sigma}_{i}]|\phi_i\rangle, \tag{7}$$

with $\rho^{\sigma}_{i}(\mathbf{r})$ being the orbital density and the projectors $\phi_i(\mathbf{r})$ being the same basis functions μ, ν used for the calculation of local occupation numbers in the LDA+U method. Above SI-correction potential differs from the original potential introduced by Filippetti and Spaldin by a factor of 1/2 which we dropped in order to obtain the exact result in the one-electron limit (*e.g.* the Hydrogen atom). The second difference between our approach and the LDA+SIC in Ref. [14] is the fact that, we use as a projector the shortest basis function (last zeta-function) instead of long-range pseudopotential. In present work,

we restricted the self-interaction correction to the d-shell only.

SIESTA treats core electrons by employing the norm-conserving pseudopotentials in their fully non-local (Kleinman-Bylander) form.[20] We generated the relativistic pseudopotentials for atomic elements using the Martins-Troullier[21] scheme with the nonlinear core corrections.[22] The electronic configurations and the cut-off radii (in a.u.), in the s/p/d/f order, were: $4s^2 4p^0 3d^7 4f^0$ and 2.0/2.0/2.0/2.0 for Co, $4s^2 4p^0 3d^8 4f^0$ and 1.7/1.88/1.88/1.88 for Ni, $5s^1 5p^0 4d^9 4f^0$ and 2.0/2.2/2.0/2.2 for Pd in the wire and 2.39/2.39/1.79/1.79 for Pd in the bulk.

The basis set adopted is a very general and flexible linear combination of numerical atomic orbitals (LCAO)[23] by Sankey and Niklewski.[24] It allows for arbitrary angular momenta, multiple-ζ, polarized and off-site orbitals. For each atom, we used an automatically generated double zeta basis set with polarization functions (which are p-type functions in the case of transition metals). The second zeta of the d-shell was used as projector function for the LDA+U and LDA+SIC operators. The radii of these projectors were (in a.u.): 1.95 for Ni, 2.073 for Co, and 2.675 for Pd. For the self-consistent calculation of the parameter U we tested in addition projector radii of 1.8 a.u. for Ni, and 2.2 a.u. for Pd.

As for the Monkhorst-Pack grid,[25] for the bulk calculations we used 20×20×20 mesh-points, and for all wires one **k**-point in the plane perpendicular to the wire and 100 **k**-points along the wire. This is good enough to represent a single nanowire in this case, in case of a very large separation between nearest neighbour nanowires. Accordingly, the distance between wires in the perpendicular plane was set to 10 Å. For the real space grid, we used a uniform mesh of quality corresponding to an energy cut-off of 400 Ry in the plane-wave method (which, in case of wires with one atom per cell, results to 2187000 mesh-points).

III. RESULTS AND DISCUSSION

A. Interatomic distances and magnetization within LSDA

The top panel of Figure 1 shows the LSDA total energy as a function of interatomic distance. Our SIESTA calculations are denoted by closed symbols and (1) in the legend. We see that for all three metals, the total energy has a well-defined minimum, which we will call the equilibrium interatomic distance. For both Ni and Co, this distance is around 2.1 Å, whereas for Pd, it is significantly larger, around 2.5 Å. Decreased coordination from 12 to 2 is of course responsible for the considerable decrease from bulk interatomic distances, 2.42 , 2.42 and 2.56 Å respectively for Ni, Co, and Pd. For comparison, we also show total energy curves obtained by other electronic-structure codes (using LDA), denoted by open symbols and (2) in the legend. For Co and Ni we plotted in particular results obtained by Smogunov *et al.* in Ref. [28] by means of plane wave method using the PWscf code;[27] for Pd we show results of an all-electron FP-LMTO (see Ref. [26] for the code) calculation, independently performed by us. As is seen, the agreement between results using the SIESTA code and other codes is more than reasonable.

The ideal breaking point a_b of a nanowire is defined as the atomic distance at which a wire under increasing stress ceases to remain locally stable and must disappear (if it did not break earlier at the wire-tip junctions as it happens in practice). This is an important parameter since in a tip-wire-tip nanocontact the very last conductance plateau before the wire breaks under increasing strain will refer to interatomic distances that are larger than equilibrium due to stress, but still have a_b as an upper limit.

As defined, the ideal breaking point a_b will coincide with the smallest interatomic distance associated with instability of some normal mode, typically with a phonon softening. While calculating the full phonon spectrum of the wire is beyond the scope of the present work, we can crudely estimate a_b in a rather simple way. In a chain held together by pairwise short range forces the longitudinal vibration branch is unstable when for increasing spacing a the interatomic restoring force is maximally negative, or equivalently, when the second derivative of the total energy is zero. Although metal nanowires are not exactly a case of pairwise short range forces, the crude estimate obtained in that approximation is sufficient for our purposes. In the middle panel of Figure 1, we plot the tension force, F, defined as

$$F = p\ A, \tag{8}$$

where p is pressure per cell and A is the surface of a plane perpendicular to the wire and restricted by the walls of the unit cell (in our case this is a hexagon with an area of 541.265877 Å^2, so the pressure of 1 kBar in a cell with 1 atom corresponds to the tension force of 5.68 nN). The force in the Pd wire is seen to have a local minimum around 2.9 Å, and the corresponding values for Ni and Co are both 2.60 Å. In the following, we will identify these distances as the ideal breaking points of the wires, keeping in mind that as explained above, they are really extreme and rough upper limits of the true breaking points. We note also that for a Pd monowire the force curve is very flat, indicating that the interatomic spacing in that system under stress should be very fluctuating.

The bottom panel of Figure 1 shows the spin magnetic moment per atom in μ_B as a function of the interatomic distance. For Pd, we also plot the magnetization calculated using the FP-LMTO code.[6] The magnetizations obtained for Ni and Co wires (filled symbols) are compared with the PWscf calculations given in Ref. [28] (open symbols). The magnetization results are summarized in Table I, where we compare them with bulk interatomic distances and magnetic moments.

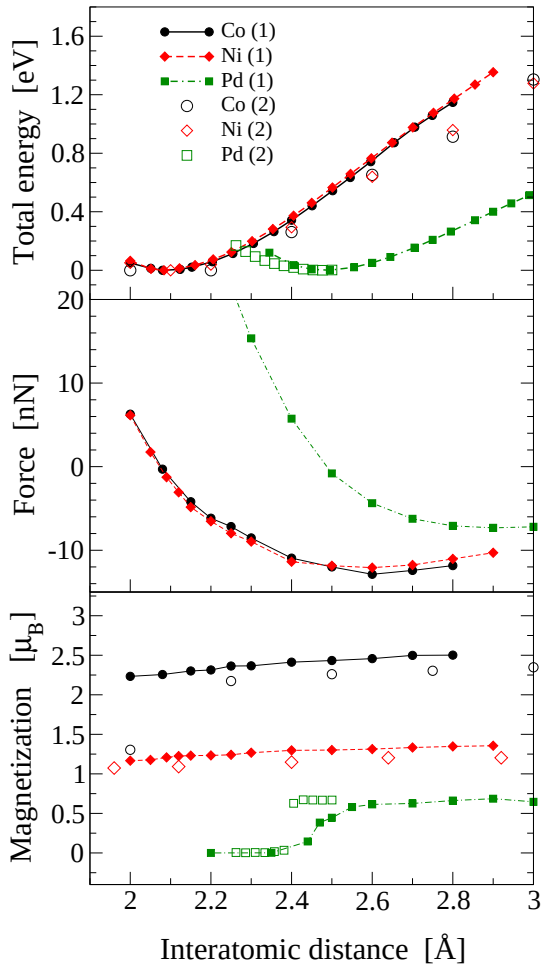

FIG. 1: Total energy, tension force and magnetization per atom for Co, Ni and Pd monowires as a function of interatomic distance. (1) denotes results obtained with the SIESTA method and (2) denotes results obtained with other methods; references are given in the text. The total energy curves for Co, Ni and Pd have been shifted, so that the minimum is at zero for all curves.

The magnetic moments for Ni and Co calculated with SIESTA are somewhat higher than these numbers calculated with the plane wave method, and than experimental bulk magnetizations. The onset of magnetism for Ni and Co wires occurs for slightly smaller interatomic distances in the SIESTA calculations compared to the PWscf calculations. For the Pd wire the magnetism occurs at slightly larger interatomic distances and appears to be more gradual than the magnetic moment calculated with the FP-LMTO code. The source of these slight discrepancies is related to differences of used pseudopotentials and the difference between the PW and LMTO schemes. SIESTA uses the normconserving PPs unlike the PWscf calculations where ultrasoft PPs were employed. We checked also the effect of using the pseudopotentials with and without nonlinear core-corrections[22] (NLCC) for magnetism. For the PPs with NLCC included, magnetism in Pd wire occured at the interactomic distance larger of about 0.2 Å.

TABLE I: Bulk and nanowire interatomic distances and magnetic moments calculated with SIESTA in LSDA. The bulk calculations were performed assuming an ideal hexagonal structure for Co, and fcc for Ni and Pd.

property	Co	Ni	Pd
interatomic distance (Å)			
bulk, this work	2.42	2.42	2.56
bulk, exp.[29]	2.51	2.46	2.67
wire equilibrium distance	2.08	2.08	2.50
wire breaking distance, a_b	2.60	2.60	2.90
magnetic moment (μ_B)			
in bulk, this work	1.95	0.63	0.0
in bulk, exp.[29]	1.72	0.61	0.0
at wire equilibrium distance	2.23	1.21	0.45
at wire breaking distance	2.46	1.32	0.69
free atom configuration	$^4F_{9/2}$	$^3F_4$	$^1S_0$

Finally, we tested the possibility of antiferromagnetic ordering in Pd, Co and Ni wires. Antiferromagnetic (AF) exchange could in principle prevail over direct ferromagnetic (FM) exchange in the extreme tight binding limit attained for very large a. We performed the AF and FM calculations with two atoms in the unit cell (to compare the total energy of two phases). We also calculated the chain of seven atoms in the unit cell, flipping the spin in the middle atom. We found that, collinear antiferromagnetic ordering is generally unstable with respect to ferromagnetic ordering, at the breaking point distance as well as for shorter interatomic distances, and in all metals studied in this work.

B. Conductance channels and magnetic moments - effect of electron correlations

A central aim of the present work is to elucidate the effect of correlations on the number of conductance channels, foreshadowing in a qualitative way the effect on ballistic conductance. In the Landauer picture of nanowire conductance, each nanowire electron band crossing the Fermi level constitutes a conducting channel between the tips at the two ends of the nanowire. Each channel can transmit electrons fully or partially, depending on a

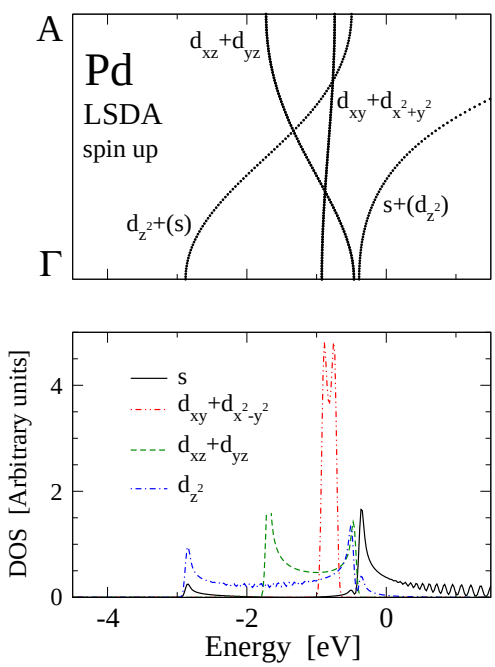

FIG. 2: Nanowire band structure with orbital labels (upper panel) and DOS (lower panel) for the majority spin of Pd obtained with LSDA at the breaking point. The Fermi level is at zero. The symmetry point A in the band-structure plot corresponds to the point $(0,0,\frac{1}{2}\ \frac{2\pi}{c})$ in the Brillouin zone.

transmission coefficient dictated by the tip-wire junction, and by the character of the electron band. In transition metals, bands with s character are generally close to total transmission. Owing to their relatively large bandwidth, s electrons are little disturbed by the potential change they experience at the tip-wire junction, and are thus essentially not reflected back, with transmission above 95%. In d-dominated channels, on the other hand, the smaller bandwidth of d states leads to higher reflection at the junction, with a much lower transmission, typically around 20% (Ref. [28]).

The d bands should of course be narrowest, and correlations strongest, for a nanowire under maximal strain. Thus, in order to investigate the effect of electron correlations on the number of conductance channels of the wires, we focus here on the nanowires electronic band structures at the breaking points. These increased interactomic distances are more similar to the conditions at which the experiments on breaking junctions have been done. Further, we identify the amount of s and d character of the bands at the vicinity of the Fermi level. This enables us to draw some qualitative conclusions regarding the conductance of the wires. In particular, it will allow a discussion of whether or not a conductance significantly below the unit conductance quantum $G_0 = 2e^2/h$ is or is not directly suggested by electron correlations, at least within the present static description.

We start by identifying the character of the bands around the Fermi level by comparing the majority spin orbital-character resolved partial density of states (DOS) with the band structure. In Figure 2, we show the band structure and s, d_{z^2}, $d_{xy} + d_{x^2-y^2}$, and $d_{xz} + d_{yz}$ partial DOS for the Pd wire at the breaking point, obtained from the LSDA calculations. In the band-structure plot, the character of the individual bands has been indicated based on information in the DOS plot. When the band is $s - d$ hybridized but one of the contributions is much smaller than the other, we show the smaller component within brackets. The band structures for Co and Ni are generally similar to that of Pd, and we refrain from repeating the same analysis over and over. For Co and Ni the character of each band can be obtained by direct comparison with Pd.

Figure 3 shows the electronic band structures for the Co, Ni and Pd wires at their respective breaking points. The left-most column shows first the standard LSDA calculation, the four middle columns the LDA+U results for a range of U between 3 eV and 9 eV, and the right-most column the results obtained in LDA+SIC. The overall effect of added correlations on the electron structures is that bands shift in energy and that the dispersion of the $s + d_{z^2}$ bands change in the vicinity of the Fermi level. The forms of the individual bands, however, are to a large degree conserved. We also see that the effects of including self-interaction corrections on the band structure are roughly similar to the effects of the LDA+U calculation with U around 3 eV or smaller.

There are quite substantial differences in the way LDA+U and LDA+SIC affect the electronic structure. The SIC potential is linearly dependent on occupation numbers. Therefore unoccupied bands do not shift, and nearly empty bands shift very little, as for example the minority spin $d_{xy} + d_{x^2-y^2}$ band in Co. On the contrary, the LDA+U approach moves unoccupied bands upwards with a constant shift $(U - J)/2$, due to the last term in Eq. (1), (see Section II). As we mentioned in the Section II, the LDA+SIC and LDA+U results may differ. This is due to the fact that LDA+SIC does not add correlations; the method removes "self-exchange" and "self-correlations". While the LDA+U method is self-interaction free within the considered shell and additionally adds correlations within this shell.

The magnetic moments of Co and Ni are largely unaffected by increased correlations, whereas the Pd moment increases substantially with U, see Table II.

In general, the properties of transition metal systems are strongly sensitive to the relative position of the s and d bands and the charge transfer between these two bands. For example, the magnetism in Pd wires is governed by $d \rightarrow s$ charge transfer.[6] Therefore, it is of interest to study the effect of correlation on the $d \rightarrow s$ transfer. Table II shows that the $d \rightarrow s$ charge transfer decreases with U for Pd (and thus in principle works toward killing off the Pd magnetism by opening up a gap), but it is

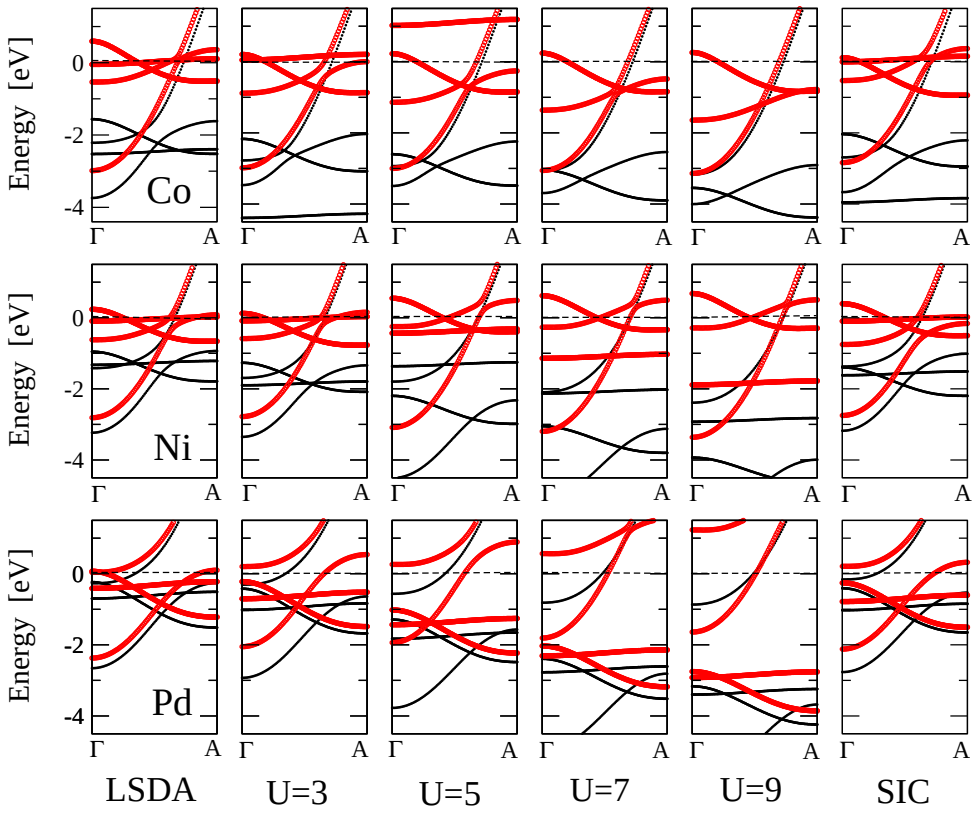

FIG. 3: Band structures of Co, Ni and Pd nanowires obtained in LSDA; in LDA+U for U = 3.0, 5.0, 7.0 and 9.0 eV and J=1.0 eV; and in LDA+SIC (d-shell only). Thin line: spin up electrons; thick line: spin down electrons; dashed line: Fermi level. All bands are plotted at the breaking point interatomic spacing a_b.

TABLE II: Properties of monatomic wires at the breaking point. M_T is the magnetic moment per atom in μ_B, M_s the spin-polarization of the s shell in μ_B, $n_s^{\uparrow+\downarrow}$ the total Mulliken occupation of the s shell, and N_c the number of spin-resolved conductance channels.

Method	Cobalt				Nickel				Palladium			
	M_T	M_s	$n_s^{\uparrow+\downarrow}$	$(N_c^{\uparrow},N_c^{\downarrow})$	M_T	M_s	$n_s^{\uparrow+\downarrow}$	$(N_c^{\uparrow},N_c^{\downarrow})$	M_T	M_s	$n_s^{\uparrow+\downarrow}$	$(N_c^{\uparrow},N_c^{\downarrow})$
LSDA	2.46	0.03	1.40	(1,6)	1.32	0.03	1.24	(1,6)	0.69	0.29	0.50	(1,4)
LDA+U (3 eV)	2.44	-0.01	1.43	(1,6)	1.32	0.03	1.24	(1,6)	0.69	0.29	0.50	(1,1)
LDA+U (5 eV)	2.43	-0.04	1.48	(1,3)	1.37	0.08	1.20	(1,4)	0.84	0.30	0.62	(1,1)
LDA+U (7 eV)	2.44	-0.04	1.48	(1,3)	1.42	0.07	1.23	(1,4)	0.96	0.22	0.80	(1,1)
LDA+U (9 eV)	2.45	-0.03	1.47	(1,3)	1.44	0.05	1.26	(1,4)	0.97	0.13	0.89	(1,1)
LDA+SIC	2.43	0.01	1.42	(1,6)	1.28	0.02	1.23	(1,5)	0.56	0.24	0.40	(1,1)

much smaller for Ni and roughly constant for Co.

In the Co wire, the largest change of the band structure when correlations are added is the upward displacement in energy of the flat nondispersive minority spin $d_{xy} + d_{x^2-y^2}$ band. The minority channel of this orbital sits right at the Fermi level in the LSDA and in LDA+SIC calculations, and it is pushed up from the Fermi level with increasing correlations within the d-shell in LDA+U. For U=7 eV and above, it is no longer visible in the band-structure plots. In contrast to that, the majority spin channel of this orbital is pushed down in energy. All remaining minority spin orbitals shift slightly down, so as to accommodate the charge transfer from the emptied minority $d_{xy} + d_{x^2-y^2}$ orbital. The corresponding majority spin bands are also downward shifted. For U=3 eV, at the band edge at A, the $d_{z^2} + (s)$ band of the minority spin channel has moved down slightly and positioned itself just on the Fermi level. For U=5 eV and larger, four

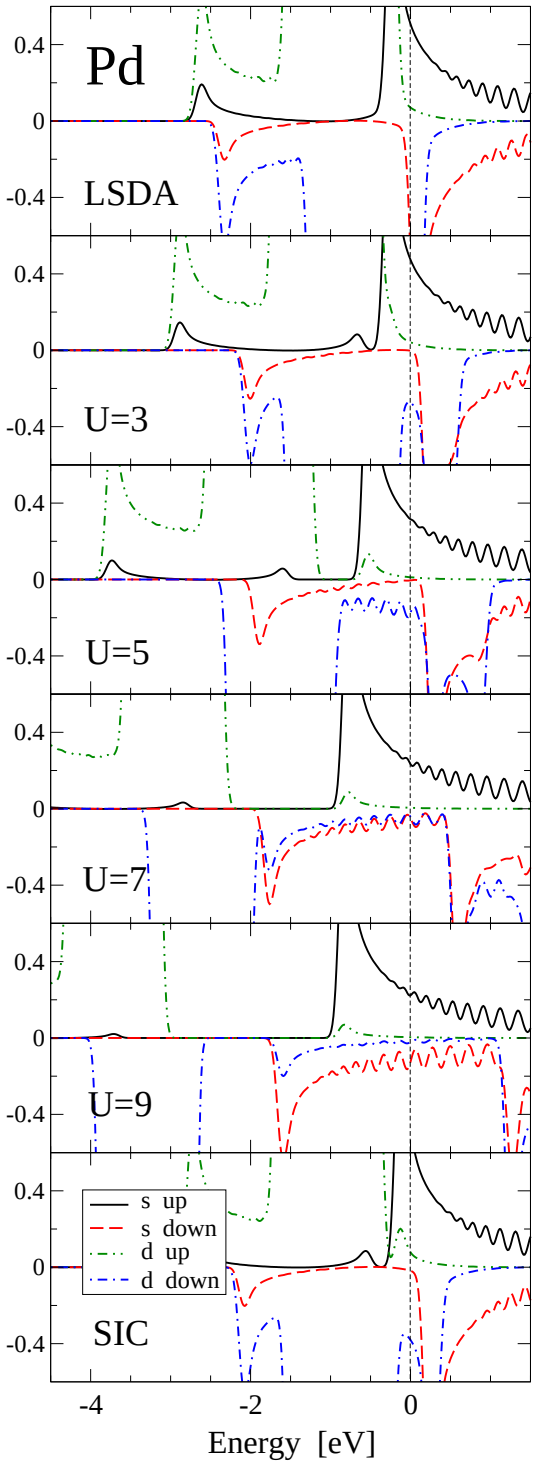

FIG. 4: Spin- and orbital-resolved s and d_{z^2} DOS for the Pd wire at the breaking point, obtained with LSDA (top panel), LDA+U (four middle panels) and LDA+SIC (bottom panel). The Fermi level is at zero.

bands cross the Fermi level: the minority spin $d_{xz} + d_{yz}$ (doubly degenerate) and the band $s+(d_{z^2})$ for both spins. The band $d_{z^2}+(s)$ for the minority spin moves down with increasing U, and gradually becomes more d-like. At the same time, the dispersion and s character of the minority spin $s + (d_{z^2})$ increases. In any case, two s channels are always open irrespective of U. The main difference between the band structure obtained with the LDA+SIC approach and the band structure for U=3 eV is that at the A edge, the minority spin band $s + (d_{z^2})$ almost do not move in case of LDA+SIC. For the other d-bands, the effect of SI is very similar to the results obtained with the LDA+U method using U of about 2-3 eV.

Ni has one more electron than Co, and consequently, in the LDA+U approach, the $d_{xy} + d_{x^2-y^2}$ (doubly degenerate) minority spin bands are now occupied and now shifted downward with increasing U, in contrast to the situation in Co. As correlations increase within the d-shell, the majority spin channels with strictly d components are pushed downward. The partly unfilled minority spin $d_{xz} + d_{yz}$ (doubly degenerate) bands of Ni move slightly upward, while the corresponding majority spin bands move down. This is consistent with a small growth of the total magnetic moment M_T, (see Table II). For the minority spin bands $s+(d_{z^2})$ and $d_{z^2}+(s)$ in Ni, one can see a similar change in dispersion to that already described for the Co wire. Also for this metal, two s channels are open at the Fermi level for all U studied. In the LDA+SIC method, the minority spin band $d_{z^2} + (s)$ moves a little bit downwards in comparison to the LSDA result, unlike the LDA+U method.

In Pd, the $d_{xy} + d_{x^2-y^2}$ bands move down with increased correlation within the d-shell, just as in Ni. Already within LSDA, these orbitals are completely filled, making the magnetic behavior of this metal very different from the one of Co and Ni. A more relevant effect of correlation in the d-shell is that the largely empty minority spin channel of the $s + (d_{z^2})$ band is pushed up, so that it becomes completely unoccupied already for U=3 eV, whereas the corresponding majority spin channel is pushed down. In the LDA+SIC band structure, the situation is similar.

Furthermore, the dispersion of the minority spin channel of the $d_{z^2} + (s)$ band increases so that this band becomes increasingly s-like with larger U. For U=3 eV or larger, only two bands cross the Fermi level, one minority spin channel and one majority spin channel, both of $s+d_{z^2}$ character, with the s character dominating. Thus, also for this metal, the two s channels remain open in all cases.

In contrast to LDA+U, the LDA+SIC results yield a smaller spin polarization relative to LSDA within the d-shell, and similar magnetization within the s-shell associated with the smaller total occupation of the s-shell.

In Figure 4, we plot the s and the d components of the DOS for spin channels in the Pd wire. In both the LSDA and LDA+SIC calculations, the s-component for both spin-channels are present at the Fermi level. In the

LDA+U scheme with U=3 eV, the minority spin at the Fermi level is dominated by the d-component and the s-component almost vanish. For larger U, the d-component decreases and the s-component grows, as discussed earlier.

Due to the aforementioned charge flow between the s- and d-shells, the magnetic moment in the s-shell decreases because the s-occupation in the majority spin is constant and the s-occupation in the minority spin increases. While the d-occupation in the minority spin decreases and the magnetic moment within the d-shell increases. The above mechanism would keep the total magnetic moment constant, but the additional contribution comes from the movement of d-bands from the Fermi level (opposite for the majority and minority spins). We stress that, the occupation within shells stems from the projected-DOS integrated over the whole energy range; therefore one should not conclude from Figure 4 that a decrease of the projected-DOS at the Fermi level is correlated with a decrease of the occupation of the projected shell.

As for the effect of correlations for the stability, we calculated the equilibrium and breaking points within LDA+U with U=5 eV for all wires. The equilibrium distances (in Å) for Co, Ni and Pd are 2.2, 2.11, 2.53 respectively, and the breaking points are 2.8, 2.63 and 2.96. The total-energy increase from the equilibrium point to the breaking point calculated within LDA/LDA+U with U=5 eV is (in eV) 0.751/0.666 for Co, 0.769/0.766 for Ni and 0.478/0.331 for Pd. The decrease of the energetic stability is mostly pronounced in Pd (about 30%) and the geometry change is the largest in the Co wire. This is somehow consistent with the band structure, because for Nickel only two bands disappear from the Fermi level when LDA+U with U=5 eV is applied while for Pd and Co wires three bands move out from the Fermi level.

All above calculations were performed with the unit cells with one atom. We also calculated chains of seven atoms in the unit cell and with the U parameter increasing when going to the middle of a cell. This way, we wanted simulate somehow the "tips"; knowing that atoms at tip surface are less correlated than atoms in a chain and more correlated than atoms in bulk.

In summary, for all three metals we find that both s channels (minority and majority spin) have finite fractional occupation for all values of U tested and also for the LDA+SIC calculations, which implies that at least the two conducting s channels are always present at the Fermi level.

IV. DISCUSSION AND CONCLUSIONS

In summary, we have found that inclusion of static repulsive electron correlations within LDA+U, while altering noticeably the electronic structure of maximally stretched monatomic transition metal nanowires, does not affect radically the number and the nature of conducting channels. In particular, a decrease is found in the (poorly conducting) d channel number (Table II), whereas the calculated number of highly conducting s channels remains in all cases one per either spin. Therefore, one quantum $G_0 = 2e^2/h$ of s conductance will be approximately preserved after adding correlations at the static level of LDA+U.

A certain reduction is predicted for the d channel conductance. At the same time, the nature of electronic states and their dispersion near E_F is also changed, which implies that tip-wire transmission should also be affected. The transmission changes are not addressed in this work, where tip-wire junctions are not explicitly included. However, because in LDA+U the filled states are lowered in energy and empty states are raised, the width of partly filled bands is somewhat larger, and that could in turn increase transmission.

Nanowire magnetism (at zero temperature) is poorly affected by correlations in Co and Ni nanowires, whereas a clear increase is predicted in Pd. Antiferromagnetism (and the associated potentially insulating state) never prevails, at least for realistic U parameters and for interatomic distances below the estimated breaking point.

It is problematic at this stage, where we have not included and treated at all the wire-tip junctions, to relate the present results to the experimentally reported ballistic conductance of Co, Ni and Pd nanocontacts. Nevertheless we can qualitatively remark that the persistence of one s channel per spin leads to expect in all cases a conductance larger than one in units of G_0. While this is in agreement with break junction observations, where the ultimate conductance jump is around 1.3 in Co (Ref. 10), 1.4 in Ni (Ref. 10), and 1.7 in Pd (Ref. 30), it does leave the fractional conductance steps $G \sim 0.5G_0$ reported in STM experiments at room temperature completely unexplained. More work, both experimental and theoretical will be needed to clarify this issue.

Acknowledgments

M.W. is grateful to Stefano de Gironcoli and Javier Junquera for discussion. We also wish to thank Ruben Weht for checking some of our results with the WIEN code[35], as well as D. Ugarte and C. Untiedt for discussions. Work in SISSA was sponsored by MIUR FIRB RBAU017S8R004, FIRB RBAU01LX5H, MIUR COFIN2003 and PRIN-COFIN2004, as well as by INFM's "Iniziativa Trasversale Calcolo Parallelo". A.D. acknowledges financial support from VR (Swedish Science Foundation).

APPENDIX A: SELF-CONSISTENT CALCULATION OF U

We calculated U self-consistently for the wires. But also, we made a scan of the wire properties as a func-

tion of U, thus, using U as a free parameter. The main reason for this was that the calculated U comes out to be very large. When calculating U self-consistently, it is important to notice that the effect of U parameter on the band shift and on the other properties, in any implementation of the LDA+U scheme, depends on the radius of the projector function, m, used to calculate the on-site occupation numbers, n_m, (see Eq. (3)). And U itself also depends on the projector radius, if it is calculated self-consistently. For smaller projector radius, calculated U is larger and the on-site occupation numbers are smaller. Therefore, the combined effect on the correction to the potential is more/less independent on the projectors.

The self-consistent U cannot be directly compared with the Hubbard-U, because the latter is defined directly by the spectroscopic properties, *i.e.* the electron affinities and the ionization potentials, as follows

$$U = E(N+1) + E(N-1) - 2E(N), \qquad \text{(A1)}$$

where E is the total energy of the system with N electrons in the considered shell. The above definition does not depend on the implementation. However, using the "exact" spectroscopic data for the U parameter could give a wrong picture, if such U was combined with the "not exact", *i.e.* projector dependent, occupation numbers. Here we want to note that, for the spectroscopic definition of U we need to use atomic configuration which involves both s- and d-shell.[32] Such calculations of U for atoms were performed for instance by Brandyopadhyay and Sarma[33] by means of the Hartree-Fock-Slater method. The phylosophy of standard LDA+U method applied in this work, however, is to correlate the electrons in the d-shell and not include the intershell interactions. Satisfying the above condition means that we cannot directly compare our U parameters with the atomic Hubbard-U, even if we abstract from the implementation and the combined effect of U and n_m.

Focusing on the solid state methods, the Coulomb parameter U can be determined from the linear response calculations with respect to a "suitable" perturbation in the occupation numbers ("suitable" means small but not too small, such that the method is sensitive to them). The details of such an approach are given in Refs. [17,18]. In this method, the U parameter is equal to

$$U = (\chi_0^{-1} - \chi^{-1})_{II}$$

where index II denotes the diagonal element at a site I, which is the atom of our interest, and the noninteracting and the interacting response functions, *i.e.* χ_0 and χ, are defined as

$$\chi_{IJ} = \frac{\partial n_I}{\partial \alpha_J}, \qquad \chi^0_{IJ} = \frac{\partial n_I}{\partial \alpha^{KS}_J}.$$

The quantity n_I is the calculated local occupation number of the considered polarization shell of the atom I. And α_I is the perturbation of the hamiltonian which enters the total energy as follows:

$$E^{KS}[\{q_I\}] = min_{n(\mathbf{r}),\alpha_I}\left\{E^{KS}[n(\mathbf{r})] + \sum_I \alpha^{KS}_I(n_I - q_I)\right\}$$

with the constrained occupation q_I. The U parameters obtained this way are given in Table III for the Ni, Co and Pd wires and for the separated atoms. For Ni and Pd, we performed the calculations at two projectors radii.

In Table III, we collect occupations and calculated U parameters. As one can see, the value of obtained U parameter decreases with increasing radius of the projector. The local occupation numbers within the d-shell, N_d, are smaller than the Mulliken ones, $N_d^{Mulliken}$. The Mulliken occupation numbers were obtained by summing over contributions from all zeta functions in the basis set and they almost do not depend on the radius of the last (smallest) zeta-function (see Eq. (4)). While the local

TABLE III: Self-consistent U and the local occupations N_d, as well as the Mulliken occupation numbers $N_d^{Mulliken}$ for the majority spin $\uparrow$ and the minority spin $\downarrow$ within the d shell, calculated for the atoms in wires and for the separated atoms.

parameters	Ni	Co	Pd
projector radius (a.u.)	1.8 / 1.950	2.073	2.2 / 2.675
Calculations for wires at the breaking point			
self-consistent U (eV)	13.9 / 12.8	12.7	9.6 / 7.6
$U\ N_d^{\uparrow}$ (eV)	56.0 / 53.5	53.0	34.8 / 31.8
$U\ N_d^{\downarrow}$ (eV)	39.1 / 37.5	25.9	30.8 / 28.5
$N_d^{\uparrow}$	4.03 / 4.18	4.17	3.62 / 4.18
$N_d^{\downarrow}$	2.81 / 2.93	2.04	3.21 / 3.75
$N_d^{\uparrow,Mulliken}$	4.91 / 4.91	4.90	4.89 / 4.89
$N_d^{\downarrow,Mulliken}$	3.53 / 3.54	2.50	4.39 / 4.43
$N_d^{\uparrow}/N_d^{\uparrow,Mulliken}$ (%)	82 / 85	85	74 / 85
$N_d^{\downarrow}/N_d^{\downarrow,Mulliken}$ (%)	80 / 83	82	73 / 85
Calculations for atoms (separation 5 Å in a chain)			
self-consistent U (eV)	16.8 / 16.2	15.6	11.1 / 10.7
$U\ N_d^{\uparrow}$ (eV)	70.4 / 70.3	66.8	40.4 / 44.5
$U\ N_d^{\downarrow}$ (eV)	41.5 / 41.6	29.3	37.3 / 43.2
$N_d^{\uparrow}$	4.19 / 4.34	4.28	3.64 / 4.16
$N_d^{\downarrow}$	2.47 / 2.57	1.88	3.36 / 4.04
$N_d^{\uparrow,Mulliken}$	5.00 / 5.00	5.00	4.98 / 4.95
$N_d^{\downarrow,Mulliken}$	3.00 / 3.00	2.19	4.60 / 4.82
$N_d^{\uparrow}/N_d^{\uparrow,Mulliken}$ (%)	84 / 87	86	73 / 84
$N_d^{\downarrow}/N_d^{\downarrow,Mulliken}$ (%)	82 / 86	86	73 / 84

occupations were summed over d-orbitals within the last zeta functions only, and these numbers depend strongly on the projector radius (see Eq. (3)). The Mulliken occupations sum to the total number of electrons in the unit cell, while the local occupations do not need to sum to total number of electrons within the d-shell because they represent only the charge around nuclei and not in the whole unit cell. Our definitions given by Eq. (3) are similar to the calculation of a charge closed within the atomic spheres in the LMTO approach (Ref. [13]). The local occupations are smaller than the Mulliken ones, by typically 20% of $N_d^{Mulliken}$.

In Table III, we give also the product UN_d (for each spin) calculated at given projector radius. We assume that, the orbital occupations, n_m, are proportional to the averaged occupations, n_d, and to the total occupations, N_d, as well. Since the deviations of orbital occupations from the averaged ones, $n_m - n_d$, are typically one or two orders of magnitude smaller than the occupation numbers n_m and n_d and N_d, the potential V_U (see Eq. (1)) is much smaller than the numbers UN_d presented in Tab. III. Nevertheless, the trend for the dependence of V_U and of UN_d on the projector radius is the same, *i.e.* very weak. Thus, we may not bother too much what projector radius we chose, because the calculated properties will not be much dependent on it, as long as it is in the reasonable range from 0.4 to 0.5 of the interatomic distance.

The calculated values of the U parameters seem to be too large. But, we will show that, these numbers give an accurate estimation of the band shift calculated with the localized basis set code. We will use data for NiO (in the rhombohedral structure with the antiferromagnetic phase) where we know exactly the experimental band gap which is 4.3 eV (Ref. 34). We calculated the fundamental gap in NiO with LSDA and LDA+U for U=2 eV and U=8 eV, and we obtained 0.22 eV, 0.69 eV, and 3.32 eV respectively, with the radius of the projector fixed at 2.5 a.u. Fitting a parabola to above results, we see that, we should use the U parameter of about 9.5 eV to obtain the experimental band gap. Such value of the U parameter is already surprisingly high, not saying about values in Tab. III if we compare them to other implementations of the LDA+U scheme.

We give some reasons for using higher U than typical values used in the plane wave approach. We rescale linearly the occupations for Ni obtained with the projector radius 1.8 a.u. and 1.95 a.u. (see Tab. III) to those (spin up and spin down) localized occupations which we would obtain using the radius of 2.5 a.u.; they would be 4.85 and 3.31 for the majority spin and the minority spin respectively. Now, if we assume that the product UN_d scales more/less linearly with the projector radius, we should take a value of about 48 for $UN_d^{\uparrow}$ and of about 34 for $UN_d^{\downarrow}$ at the radius of 2.5 a.u. Dividing these numbers by the expected occupations at that projector radius, we will obtain the U parameters of about 9.9 eV and 10.2 eV for the majority spin and the minority spin respectively. Which gives in average about 10 eV. We know that the U parameter should be larger for the atom than for the bulk. Thus for the wire, a value of 10 eV is quite good in a comparison to its bulk value of 9.5 eV. This way, using the experimental data for a band gap in NiO and a fit for our numerical data obtained with LSDA and LDA+U with U=2 and U=8 eV, and rescaling results for Ni wire to the expected result for a larger projector radius, we obtained two very close values of the U parameter for Ni. The result of above procedure is the proof that one could use the parameters presented in Table III and that obtained this way band shifts in wires would be correct.

On the other hand, the band shift is not the only property one would like to get from the LDA+U scheme. For instance, the correct orbital ordering in NiO could be obtained with a smaller value of U, about 6 eV. Therefore, for the sake of the balance between different properties which we want to describe, we take a bit smaller values of U than these which give the expected band shifts in bulk.

At the end we conclude that, for the number of channels crossing the Fermi level, it is not very important how large U we take, because for U about 3∼4 eV the bands which are supposed to move already have done it.

[1] H. Ohnishi, Y. Kondo, and K. Takayanagi, Nature, **395**, 780 (1998).

[2] V. Rodrigues, T. Fuhrer, and D. Ugarte, Phys. Rev. Lett. **85**, 4124 (2000).

[3] Y. Oshima, A. Onga, and K. Takayanagi, Phys. Rev. Lett. **91**, 205503 (2003).

[4] A. I. Yanson, G. R. Bollinger, H. E. van den Brom, N. Agraït, and J. M. van Ruitenbeek Nature (London) **395**, 783 (1998).

[5] D. Spišák and J. Hafner, Comp. Mat. Sci. **27**, 138 (2003); D. Spišák and J. Hafner, Phys. Rev. B **67**, 214416 (2003).

[6] A. Delin, E. Tosatti, and R. Weht, Phys. Rev. Lett. **92**, 057201 (2004); A. Delin and E. Tosatti, J. Phys. Cond. Mat. **16**, 8061 (2004).

[7] A. Delin and E. Tosatti, Phys. Rev. B **68**, 144434 (2003); A. Delin and E. Tosatti, Surface Science **566-568**, 262 (2004).

[8] S. R. Bahn and K. W. Jacobsen, Phys. Rev. Lett. **87**, 266101 (2001).

[9] V. Rodrigues, J. Bettini, P. C. Silva, and D. Ugarte, Phys. Rev. Lett. **91**, 096801 (2003).

[10] C. Untiedt, D. M. T. Dekker, D. Djukic, and J. M. van Ruitenbeek, Phys. Rev. B **69**, 081401 (2004).

[11] T. Ono, Y. Ooka, H. Miyajima, and Y. Otani, Appl. Phys. Lett. **75**, 1622 (1999).

[12] P. Hohenberg and W. Kohn, Phys. Rev. **136**, B864 (1964); W. Kohn and L. J. Sham, Phys. Rev. **140**, A1133 (1965).

[13] V.I. Anisimov, J. Zaanen, and O.K. Andersen, Phys. Rev.

B **44**, 943 (1991); V. I. Anisimov, F. Aryasetiawan, and A. I. Lichtenstein, J. Phys. Cond. Mat. **9**, 767 (1997).
[14] A. Filippetti and N. A. Spaldin, Phys. Rev. B **67**, 125109 (2003).
[15] J. M. Soler, E. Artacho, J. D. Gale, A. Garcia, J. Junquera, P. Ordejon and D. Sanchez-Portal, J. Phys. Cond. Matter **14**, 2745 (2002); www.uam.es/departamentos/ciencias/fismateriac/siesta
[16] M. Wierzbowska, D. Sánchez-Portal and S. Sanvito, Phys. Rev. B **70**, 235209 (2004).
[17] M. Cococcioni and S. de Gironcoli, Phys. Rev. B **71**, 035105 (2005).
[18] P. H. Dederichs, S. Blügel, R. Zeller and H. Akai, Phys. Rev. Lett. **53**, 2512 (1984).
[19] M. Wierzbowska, D. Sánchez-Portal and S. Sanvito, (in press).
[20] L. Kleinman and D. M. Bylander, Phys. Rev. Lett. **48**, 1425 (1982).
[21] N. Troullier and J. L. Martins, Phys. Rev. B **43**, 1993 (1991).
[22] Louie, Froyen, Cohen, Phys. Rev. B **26**, 1738 (1982).
[23] J. Junquera, O. Paz, D. Sánchez-Portal and E. Artacho, Phys. Rev. B **64**, 235111 (2001); E. Anglada, J. M. Soler, J. Junquera and E. Artacho, Phys. Rev. B **66**, 205101 (2002); E. Artacho, D. Sánchez-Portal, P. Ordejón, A. García and J. M. Soler, Phys. Stat. Solidi B **215**, 809 (1999).
[24] O. F. Sankey and D. J. Niklewski, Phys. Rev. B **40**, 3979 (1989).
[25] H. J. Monkhorst and J. D. Pack, Phys. Rev. B **13**, 5188 (1976).
[26] J. M. Wills, O. Eriksson, M. Alouani, and O. L. Price, in *Electronic Structure and Physical Properties of Solids*, edited by H. Dreyssé (Springer, Berlin, 2000).
[27] S. Baroni, A. Dal Corso, S. de Gironcoli and P. Giannozzi, www.pwscf.org
[28] A. Smogunov, A. Dal Corso, and E. Tosatti, Surf. Science **507**, 609 (2002); A. Smogunov, A. Dal Corso, and E. Tosatti, Surf. Science **532**, 549 (2003); A. Smogunov, A. Dal Corso, and E. Tosatti, Phys. Rev. B **70**, 045417 (2004).
[29] N. W. Ashcroft and N. D. Mermin, *Solid state Physics* (Saunders College/Philadelphia) 1976.
[30] Sz. Csonka, A. Halbritter, G. Mihály, O. I. Shlyarevskii, S. Speller and H. van Kempen, Phys. Rev. Lett. **93**, 016802 (2004).
[31] R. S. Mulliken, J. Chem. Phys. **23**, 1833 (1955); R. S. Mulliken, J. Chem. Phys. **23**, 1841 (1955).
[32] R. D. Cowan, *The theory of atomic structure and spectra* (University of California Press/London, England) 1981.
[33] T. Brandyopadhyay and D. D. Sarma, Phys. Rev. B **39**, 3517 (1989).
[34] A. Fujimori and F. Minami, Phys. Rev. B **30**, 957 (1984).
[35] P. Blaha, K. Schwarz, and J. Luitz, computer code WIEN97 (Vienna University of Technology, Vienna, 1997), [Improved and updated UNIX version of the original copyrighted WIEN code, which was published by P. Blaha, K. Schwarz, P. Sorantin, and S. B. Trickey, Comput. Phys. Commun. **59**, 339 (1990)].